Progress in optical devices and materials

GGC
2007
PRO

technische universiteit eindhoven

2007 Annual Workshop of the IEEE LEOS Benelux Chapter

Supported by

COBRA

Progress in Optical Devices and Materials

IEEE LEOS
LASERS & ELECTRO-OPTICS SOCIETY

Editors

B. Huiszoon, P.J. Urban, C. Caucheteur

May 25, 2007

COBRA Institute

Eindhoven University of Technology

The Netherlands

PROCEEDINGS 2007

Annual Workshop of the IEEE/LEOS Benelux Chapter

Progress in Optical Devices and Materials

Friday May 25, 2007
COBRA Institute
Eindhoven University of Technology
The Netherlands

Editors
B. Huiszoon, P.J. Urban, C. Caucheteur

Organized by
IEEE/LEOS Benelux Student Chapter
in association with IEEE/LEOS Benelux Chapter

Published by IEEE/LEOS Benelux Chapter
Eindhoven University of Technology
Department of Electrical Engineering
Division of Telecommunication Technology and Electromagnetics
Den Dolech 2
P.O. Box 513
5600 MB Eindhoven
The Netherlands

Phone +31 (0)40 2473451
Fax +31 (0)40 2455197
www http://tte.ele.tue.nl
www http://leosbenelux.org

Keywords integrated optics, photonics, lasers, lightwave technology, non-linear optics, optical communication, optical materials, photonic crystals, nanophotonics, quantum electronics

---

CIP-DATA LIBRARY TECHNISCHE UNIVERSITEIT EINDHOVEN

IEEE/LEOS

IEEE/LEOS Benelux Chapter : annual workshop proceedings, progress in optical devices and materials, May 25, 2007, Eindhoven, The Netherlands / editors: B. Huiszoon, P.J. Urban and C. Caucheteur - Eindhoven : Technische Universiteit Eindhoven, 2007.
ISBN 978-90-6144-987-4
NUR 959
Trefw.: geintegreerde optica / optische telecommunicatie / fotonica / lasers.
Subject headings: integrated optics / optical communication / microwave photonics / lasers.

Preface

This year it is the privilege of Eindhoven University of Technology to host the eleventh Annual Workshop of the IEEE/LEOS Benelux Chapter. The workshop is organized by the Student Chapter. We took the initiative this year to bundle the contributions and to publish proceedings.

The fields of interest of the Lasers and Electro-Optics Society are lasers and integrated optics, optical fibers, optical communication systems and devices, optical sensors, physics of novel materials, polymers and inorganic materials, non-linear optics, quantum electronics and quantum optics.

The Benelux Chapter was founded in 1996 with the main objective to promote the LEOS fields in the Benelux as well as in the neighbouring countries Germany and France, by stimulating interactions between scientists and engineers working in universities, industry and other research institutes. The Society is concerned with the research, development, design, manufacture, and applications of materials, devices and systems, and with the various scientific and technological activities, which contribute to the useful expansion of the field of quantum electronics and of its applications. A special attention is paid to the students to reinforce strong scientific and human collaboration between universities and industries.

Few years ago, all the activities related to students were organized by the IEEE/LEOS Benelux Chapter Board, especially by the two student members of this board. This was not an ideal situation in terms of visibility and manpower and thus, Marc Sciamanna and Douwe Geuzebroek initiated a call for participation for a separate Student Chapter within the Benelux.

The Student Chapter was then founded in 2004 to have a better visibility of the student activities within the region. Furthermore a board consisting out of students can organize more activities, since more students can be involved. The Student Chapter was thus created to support the formal and informal acquaintance between the (PhD) students working in the field of LEOS within the Benelux. Currently, the student board has twelve volunteers from almost all universities dealing with the fields covered by the LEOS.

The Workshop has been organized yearly since 1996 and it is now the most prominent event of the Student Chapter. It provides an excellent forum for young scientists to exchange their latest results and to promote the research going on in the Benelux region to a wide public. The 2007 Workshop is a one day event that comprises two invited contributions and ten oral contributions. This year we are particularly proud to welcome a LEOS Distinguished Lecturer professor Bishnu P. Pal from the Indian Institute of Technology Delhi, New Delhi, India who will give an invited talk on guided wave optical components entitled "Microstructured Optical Fibers: An Emerging Technology and its Potentials". It has become a tradition to invite an excellent PhD student from a

university of the Benelux to give a presentation. The junior invited speaker of this edition is Gunther Roelkens from Ghent University. His talk is entitled "Heterogeneous III-V/Silicon Photonics: Bonding Technology and Integrated Devices".

The Workshop organizing committee would like to thank the invited speakers and presenters of regular papers for their valued contributions. This kind of interaction constitutes the spirit of our Student Chapter. We also thank the Program Committee and the volunteers who helped to put this Workshop together. Finally we would like to acknowledge the support from our sponsors. Without their contribution, the organization of this Workshop would not have been possible.

On behalf of the Workshop organizing committee,

LEOS Benelux Student Chapter
May 25, 2007

Technical Program Committee

Prof. Peter Bienstman	Universiteit Gent
Prof. Jan Danckaert	Vrije Universiteit Brussel
Dr. Fouad Karouta	Technische Universiteit Eindhoven
Prof. Daan Lenstra	Technische Universiteit Delft
Dr. René de Ridder	Universiteit Twente
Dr. Marc Wuilpart	Faculté Polytechnique de Mons

Organizing Committee

Christophe Caucheteur MSc., chairman
Jonathan Bradley MSc., vice-chairman
Philippe Tassin MSc., secretary
Ronald Dekker PhD., treasurer
Toh Kee Chua MSc.
Cathy Crunelle MSc.
Dimitri Geskus MSc.
Bas Huiszoon MSc.
Milan Marell MSc.
Wouter van Parys MSc.
Patryk Urban MSc.
Katrien de Vos MSc.

Contents

Microstructure Optical Fibers: An Emerging Technology and its Potentials

Bishnu Pal

Indian Institute of Technology Delhi
Physics Department
New Delhi: 110 016, India

Consequent to the mind boggling progress in high-speed optical telecommunication witnessed in late 1990s, it appeared that it would only be a matter of time before the huge theoretical bandwidth of 53 THz, offered by low-loss transmission windows (extending from 1280 nm to 1650 nm) in low water peak high-silica optical fibers would be tapped for telecommunication through dense wavelength division multiplexing techniques! In spite of this possibility, there has been a considerable resurgence of interest amongst researchers to develop application-specific specialty fibers, e.g. fibers in which transmission loss of the material would not be a limiting factor and in which nonlinearity and dispersion properties could be conveniently tailored to achieve transmission characteristics that are otherwise almost impossible to realize in conventional high-silica fibers. Research targeted at such fiber designs in the early 1990s gave rise to a new class of fibers, known as microstructured optical fibers (MOFs), which are characterized with wavelength scale periodic refractive index features. These structures exhibit photonic bandgaps i.e these forbid propagation of a certain band of wavelengths within them. If the frequency of incident light happens to fall within the photonic bandgap, which is characteristic of these fibers, then propagation of light is forbidden inside it. In contrast to the electronic bandgap, which is a consequence of a periodic arrangement of atoms/molecules in a semiconductor crystal lattice, a photonic bandgap arises due to a periodic distribution of refractive index in a PCF. However by introducing in the central region a defect to an otherwise periodic structure, light (within the bandgap) could be localized in the defect region thereby mimicking a fiber core. The defect region could be a medium of refractive index higher or lower (e.g. air) than the average refractive index of the surrounding layers. In case of lower refractive index defect, the corresponding MOFs are known as photonic bandgap fibers (PBGFs). In contrast to a conventional optical fiber, in which light is guided by total internal reflection, Bragg scattering is responsible for effective wave guidance in such fibers, which led to the christening of these fibers as photonic bandgap guided optical fibers. In 1987, Yablonovitch and John independently proposed for the first time the possibility of controlling properties of light through the photonic bandgap effect in man-made photonic crystals. Microstructured optical fibers have been a fall out of that research. The talk would focus on basic functional principle of optical wave guidance in such fibers vis-a-vis conventional fibers. Details of propagation and design & technology of 1D photonic band gap Bragg fibers would be described, in which we have recently made some research contributions and our collaborators in Russian Academy of Science have succeeded in fabricating some of our designed fibers. Discussions on applications would include designs of dispersion compensating fibers, fibers for metro networks, generation of supercontinuum light, and possibly on Bragg reflection waveguides.

Heterogeneous III-V/Silicon Photonics: Bonding Technology and Integrated Devices

G. Roelkens, J. Brouckaert, J. Van Campenhout, D. Van Thourhout, R. Baets

Photonics Research Group, INTEC, Ghent University
Sint-Pietersnieuwstraat 41,
B-9000 Ghent – Belgium
Gunther.Roelkens@intec.UGent.be

In this paper we give an overview of our research in the field of III-V/silicon photonics. The technology for integrating high-quality III-V layers on top of silicon-on-insulator waveguide circuits will be outlined together with the realization of laser diodes and photodetectors in this III-V layer.

Heterogeneous III-V/Silicon photonics

While silicon-on-insulator (SOI) is nowadays used for the fabrication of high-end electronic integrated circuits, the use of the material system for photonic applications is intensively studied. A silicon-on-insulator wafer (commercially available up to 300mm in diameter) consists of a silicon layer on top of a buried SiO_2 layer, fabricated on a silicon substrate. While in electronic integrated circuits the presence of the buried SiO_2 layer improves transistor performance, in photonic applications it is used to create a high vertical refractive index contrast between the silicon top layer (n_{Si}=3.45) and the SiO_2 (n_{SiO2}=1.45), to be able to guide near-infrared light (λ>1.1μm) in the silicon top layer by total internal reflection. A large omni-directional index contrast can be obtained by laterally etching the silicon top layer to obtain a silicon photonic wire surrounded by a low refractive index air and SiO_2 cladding. In order to restrain the propagation of light in the optical waveguide to a single optical mode at the telecommunication wavelengths of 1.3 and 1.55μm, a typical maximum waveguide cross-section of 0.1μm^2 is required. The high omni-directional refractive index contrast enables large-scale integration of optical functions on an SOI chip, as light is tightly confined to the silicon wire. It allows the fabrication of ultra-compact resonators with high quality factor, wavelength-scale waveguide bends and optical circuits with photonic wire pitches on the order of 1μm with negligible crosstalk. Moreover, the tight confinement –and the associated high power densities- in the photonic wire allows exploiting the nonlinear optical properties of silicon at moderate optical power levels. To fabricate these photonic integrated circuits, standard CMOS technology can be used [1]. This allows high-yield fabrication and a reduction of the component cost by the economy of scale. Even the integration of photonic and electronic functions on a common substrate is feasible. Although in recent years many research groups reported high-performance operation of photonic circuits in SOI (both passive optical functions like wavelength-selective optical functions, optical power splitters, etc. and active optical functions like optical modulators and all-optical wavelength converters), the use of silicon as a medium for stimulated light emission is hampered by the indirect band gap of silicon. Due to this indirect band gap, the probability for an excited electron-hole pair to recombine and emit a photon is strongly reduced due to the much higher non-radiative recombination rate. Although several advances are being made to achieve light

emission from silicon, either by modifying the silicon material on a nano-scale [2] or by exploiting its nonlinear optical properties [3], in the foreseeable future these devices will not outperform their III-V semiconductor counterparts, supplying state-of-the-art opto-electronic components for the telecommunication market nowadays. Therefore, we propose to integrate a direct band gap III-V layer on top of the silicon-on-insulator waveguide substrate to achieve stimulated light emission and to couple this stimulated emission to the underlying SOI waveguide circuit. This III-V layer can at the same time be used as a photodetection layer. The integration process should however maintain the advantages of the CMOS manufacturing process, namely the high yield and the economy of scale.

Bonding Technology

In order to achieve the heterogeneous integration of a III-V layer on top of an SOI waveguide circuit, a DVS-BCB adhesive die-to-wafer bonding process was developed [4]. In DVS-BCB adhesive wafer bonding, an oligomer solution of DVS-BCB is spin coated on the processed SOI waveguide circuit. This spin coating process planarizes the waveguide topography. After spin coating, a baking step at 150C removes the residual solvent in the spin coated film while a short baking step at 250C transforms the liquid DVS-BCB to a sol/gel rubber by partial polymerization of the DVS-BCB. The preparation of the InP/InGaAsP epitaxial layer surface was optimized to achieve a high bonding strength. A HF surface treatment improved the bonding strength by chemical modification of the III-V surface. After attachment of the III-V dies, the wafer stack is cured at 250C for 1 hour to completely polymerize the DVS-BCB. A uniform pressure is applied to the wafer stack during curing to achieve an intimate contact between both surfaces . DVS-BCB was chosen as bonding agent due to its optical transparency, its excellent planarization properties, its low curing temperature, the fact that no outgassing occurs during cure and its high glass transition temperature (>350C), determining the available post-bonding thermal budget for the fabrication of the laser diodes and photodetectors. After bonding, the InP growth substrate is removed using a combination of mechanical grinding and wet chemical etching using $HCl:H_2O$ until an InGaAs etch stop layer is reached.

Integrated devices

Several types of photodetectors and laser diodes were fabricated in the bonded III-V epitaxial layer and coupling between the III-V layer and the underlying SOI waveguide substrate was demonstrated. Laser light from a bonded InP/InGaAsP Fabry-Perot laser diode was coupled to the SOI waveguide circuit using an inverted adiabatic taper approach as shown in figure 1a. 1mW of optical power was coupled to the SOI waveguide circuit. The detrimental influence of the high thermal resistivity of the bonded laser diodes due to the polymer bonding layer was tackled by incorporating an integrated heat sink structure, as will be discussed during the workshop. The same coupling approach and type of device was used as a photodetector. A device responsivity of 0.22A/W was obtained at 1550nm [5]. While this type of device layout allows to use the same processing and epitaxial layer structure to fabricate laser diodes and photodetectors together on an SOI waveguide circuit, the number of processing steps are relatively large. For applications only requiring an array of photodetectors, a

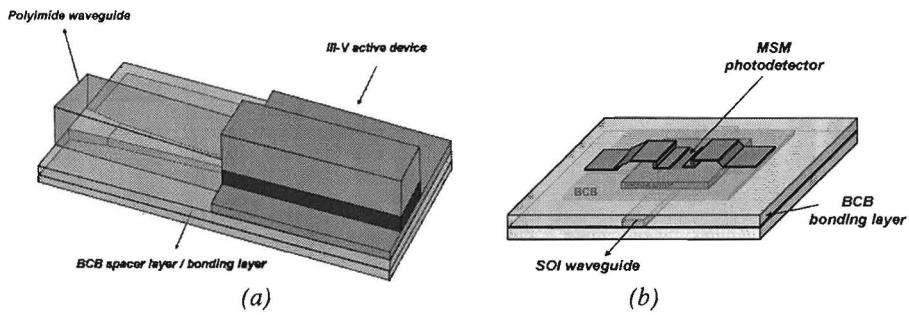

Figure 1: Layout of the III-V devices integrated on top of the SOI waveguide circuit. A Fabry-Perot laser diode/photodetector structure (a) and an MSM photodetector structure (b)

new type of waveguide-coupled InAlAs/InGaAs MSM (metal-semiconductor-metal) photodetector was designed and fabricated as shown in figure 1b. Coupling of light from the SOI waveguide into the photodetector structure is achieved through a vertical directional coupling mechanism. Device responsivities of 1A/W were obtained at 1550nm, while device processing is easier compared to the pin-type photodetector structure [6]. While these types of devices (and associated bonding technology) will be discussed in detail during the workshop, other types of integrated laser diodes and photodetector devices will be outlined as well.

Applications

Several applications could emerge from this technology. Especially in those applications where a combination of active and passive optical functions is required and where cost is an important factor, heterogeneous III-V/silicon photonics can have an large impact. For example, in applications like fiber-to-the-home, the next broadband network, where each end-user requires a transceiver for (de)multiplexing, transmitting and receiving optical signals and where low-cost components are required in order to boost the deployment of these networks, III-V/silicon photonic components can be of large interest.

References

[1] Bogaerts, W., et al., *Nanophotonic waveguides in silicon-on-insulator fabricated with CMOS technology.* Journal of Lightwave Technology, 2005. **23**(1): p. 401-412.
[2] Pavesi, L., *Will silicon be the photonic material of the third millenium?* Journal of Physics-Condensed Matter, 2003. **15**(26): p. R1169-R1196.
[3] Rong, H.S., et al., *Monolithic integrated Raman silicon laser.* Optics Express, 2006. **14**(15): p. 6705-6712.
[4] Roelkens, G., et al., *Adhesive bonding of InP/InGaAsP dies to processed silicon-on-insulator wafers using DVS-bis-benzocyclobutene.* Journal of the Electrochemical Society, 2006. **153**(12): p. G1015-G1019.
[5] Roelkens, G., et al., *Laser emission and photodetection in an InP/InGaAsP layer integrated on and coupled to a silicon-on-insulator waveguide circuit.* Optics Express, 2006. **14**(18): p. 8154-8159.
[6] Brouckaert, J. et al., *Thin film III-V photodetectors integrated on silicon-on-insulator photonic ICs,* Journal of Lightwave Technology, to be published

Experimental study of $Nd(TTA)_3Phen$-doped 6-FDA/Epoxy Waveguides

J. Yang, M.B.J. Diemeer, L.T.H. Hilderink, and A. Driessen

University of Twente, Integrated Optical Microsystems Group, P.O. Box 217, Enschede, the Netherlands

The infrared fluorescence (890nm, 1060nm, 1330nm) of a $Nd(TTA)_3Phen$ (TTA = thenoyltrifluoroacetone, Phen = 1, 10-phenanthroline) doped 6-FDA epoxy (6-fluorinated-dianhydride cured epoxy) film was observed by pumping with a Ti:Sapphire laser at 800nm. Furthermore, $Nd(TTA)_3Phen$ doped 6-FDA epoxy channel waveguides were fabricated and their loss spectrum was measured.

Introduction

Lasing and amplification by rare-earth doped polymer materials has been widely investigated [1-2]. In our previous work [3], a $Nd(TTA)_3$phen doped 6-FDA epoxy film was spin-coated on an thermally oxidized wafer. The Judd-Ofelt analysis based on the absorption spectrum shows that this neodymium doped polymer material has a good potential to be used as a planar waveguide in lasers or amplifiers.

In this paper, the spontaneous emission spectrum of this neodymium doped film and the fabrication of $Nd(TTA)_3$phen doped 6-FDA epoxy channel waveguides by backfilling the core material in inverted cladding channels are presented.

Spontaneous emission spectrum of neodymium doped film

The absorption spectrum of $Nd(TTA)_3$phen doped 6-FDA epoxy film, which is obtained in our previous work [3], indicates the absorption peaks at 580nm, 740nm, 800nm and 865nm.

Therefore, the recording of the room temperature fluorescence spectrum was performed using the 800 nm line of a tunable Ti:Sapphire laser as the excitation source. The spontaneous emission spectrum was recorded by an optical spectrum analyzer (Spectro 320, Instrument System) and is shown in Fig. 1 Three distinct emission bands with peaks at 890 nm, 1060nm and 1330nm can be seen clearly. They correspond to transitions from the $^4F_{3/2}$ level to the $^4I_{9/2}$, $^4I_{11/2}$, and $^4I_{13/2}$ levels.

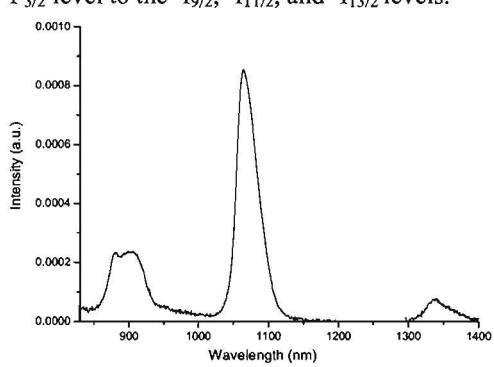

Fig. 1 Room temperature spontaneous emission of the Nd(TTA)3phen doped 6-FDA epoxy film pumped by Ti:Sapphire laser at 800nm.

Waveguide fabrication and loss measurement

By spin-coating and photodefining a cycloaliphatic epoxy prepolymer (code name CHEP) [4], inverted channels in the low index CHEP polymer were obtained on a thermally oxidized wafer. The core material, a $Nd(TTA)_3phen$ doped 6-FDA epoxy solution, was then backfilled via spin-coating twice and the Nd doped channel waveguide was realized after thermal curing. A lower refractive index silicon containing epoxy was used as the upper cladding, and on the top of which a Pyrex glass wafer was applied. Fig. 2 shows a microscope picture of the waveguide cross section (~40 μm).

The waveguide loss was determined from the optical output of samples with different lengths using butt-coupled 50 μm multimode fibers, a broadband white light source at the input and the Spectro 320 at the output. The loss spectrum clearly shows the absorption lines of the neodymium, which appear at 580, 740, 800 and 865 nm (Fig. 3).

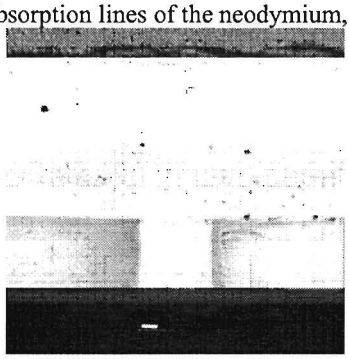

Fig. 2 Microscope picture of the Nd doped channel waveguide cross-section.

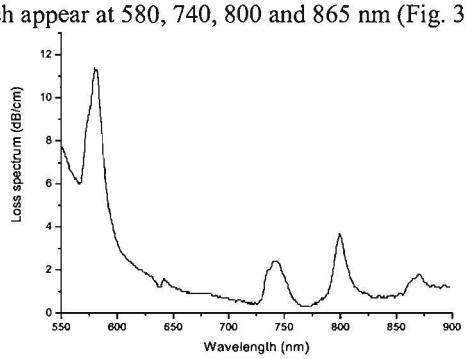

Fig. 3 Loss spectrum of the $Nd(TTA)_3phen$ doped 6-FDA epoxy channel waveguide.

Conclusion

Spontaneous emission spectrum of the neodymium doped polymer film with three peaks at 890nm, 1060nm and 1330nm was obtained. Channel waveguides were realized by backfilling the inverted channels in a low index epoxy with the core material and their loss was measured. This study demonstrates that $Nd(TTA)_3Phen$ doped 6-FDA epoxy is well suited for lasing or amplification in optical waveguides.

Acknowledgement

The authors acknowledge the financial support of STW (TOE 6986).

References

[1] S. Lin, R. J. Feuerstein, and A.R. Mickelson, "A study of neodymium-chelate-doped optical polymer waveguides", J. Appl. Phys., vol. 79, pp.2868-2874, 1996.

[2] K. Kueki and Y. Koike, "Plastic optical fiber lasers and amplifiers containing lanthanide complex", Chem. Rev., vol 102, pp. 2347-2356, 2002.

[3] J. Yang, M.B.J. Diemeer, L.T.H. Hilderink, R. Dekker, and A. Driessen, "Judd-Ofelt analysis of $Nd(TTA)_3phen$ doped 6-FDA/epoxy planar waveguides," in Proceedings of the Annual Symposium of the IEEE/LEOS Benelux Chapter 2006, pp. 253-256.

[4] M.B.J. Diemeer, L.T.H. Hilderink, H. Kelderman, and A. Driessen, "Multimode waveguides of Photodefinable epoxy for optical backplane applications," in Proceedings of the Annual Symposium of the IEEE/LEOS Benelux Chapter 2006, pp. 53-56.

Polarization based filtering in a wavelength converter

L.M. Augustin, J.J.G.M. van der Tol, M.K. Smit

COBRA Research Institute, Technische Universiteit Eindhoven
Postbus 513, 5600 MB Eindhoven, The Netherlands

A new scheme is demonstrated to filter signals after a wavelength converter based on integrated polarization components. This allows polarization independent conversion, co-propagating operation without a tuneable filter, and it facilitates conversion to the same wavelength.

Introduction

Wavelength converters are key-components in future optical networks. Wavelength converters experience some problems: polarization dependent operation, need for expensive tuneable filters and problems in converting to the same wavelength.
The POLARIS (POlarisation LAbelling for Rejection and Isolation of Signals) wavelength converter can deal with these problems.

Principle

The concept of POLARIS is depicted in Fig. 1. The signal from the network arrives in an arbitrary polarization. This signal is split in the polarization splitter (PS) into two orthogonal polarizations. In one branch, the polarization is rotated in the polarization converter (PC) to have the signal in both branches in the same polarization (TE). These signals are injected into the Mach Zehnder Interferometers (MZI) together with the locally generated CW light in the orthogonal polarization (TM). After interacting in the MZI the signal is transferred to the CW wavelength and both signals have to be separated. This is done by rotating the polarization of the upper branch and then using a PS to combine both branches. As only TE in the upper and TM in the lower input will couple to the output, filtering of the unwanted signal occurs. Simulations show polarization independent behavior and promising BER, ER and isolation [1]. All components (MZI,

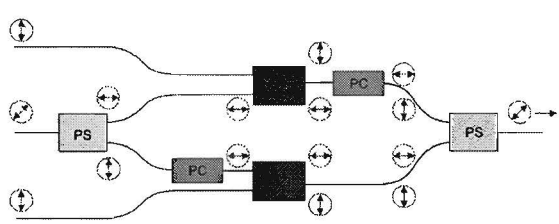

Figure 1: Schematic of the POLARIS wavelength converter

PC, PS) can be monolithically integrated. The polarization components will be treated below.

Polarization converter

An improved design for a PC is proposed (Fig. 2(a)) that uses the same topcladding as an active device and can be integrated with the other components [2]. It consists of a

waveguide with a vertical and a slanted side. Because of the latter, the modes in the converter are tilted. Both modes are excited when either TE or TM polarized light is input. After half a beatlength the two modes are completely out of phase and recombine in the orthogonal polarization.
The maximum conversion from TE to TM and vice versa (for this device 97.5%) occurs at 131 μm length, and back to zero at the full beat length (Fig. 2(c)).

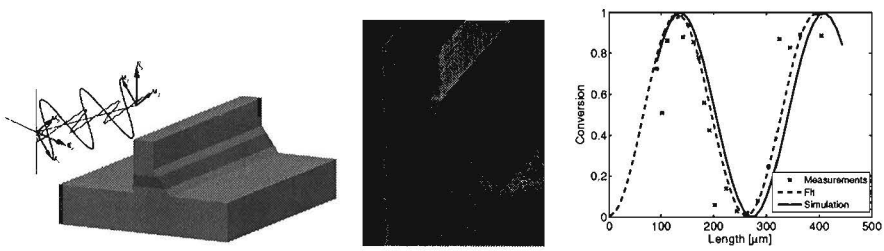

(a) Schematic overview (b) SEM photograph (c) Measured conversion

Figure 2: Polarization converter

Polarization splitter

A short (600 μm long), interference based splitter integrated with a polarization converter is demonstrated. The device consists of a Mach Zehnder Interferometer with polarization converters in both arms (Fig. 3) [3].
The device is fabricated and first measurements show a splitting of 10 dB and a conversion of 90 %.

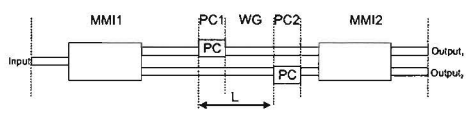

Figure 3: Schematic of the MZI polarization splitter/converter

Conclusions

An improved scheme for filtering in wavelength conversion is shown. Polarization components needed for monolithic integration are demonstrated. Polarization conversion up to 97.5% is shown, polarization splitting of 10 dB is achieved.

References

[1] R. Hanfoug, J. J. G. M. van der Tol, L. M. Augustin, and M. K. Smit. Wavelength conversion with polarisation labelling for rejection and isolation of signals (POLARIS). In *Proc. 11th Eur. Conf. on Int. Opt. (ECIO '03)*, pages 105–108. Prague, Czech Republic, April 2–4 2003.

[2] L.M. Augustin, J.J.G.M. van der Tol, and M.K. Smit. A compact passive polarization converter for active-passive integration on InP/InGaAsP. In *Proc. 13th Eur. Conf. on Int. Opt. (ECIO '07)*, Copenhagen, Denmark, April 25–27 2007.

[3] L.M. Augustin, J.J.G.M. van der Tol, R. Hanfoug, W.J.M. de Laat, and M.K. Smit. An integrated polarization splitter and converter. In *Proc. IEEE/LEOS Symposium (Benelux Chapter)*, pages 89–92. Eindhoven, The Netherlands, December 2006.

Silicon-on-Insulator Microring Resonator for Biosensing

K. De Vos, I. Bartolozzi, E. Schacht, P. Bienstman and R. Baets

IMEC-INTEC Photonics Research Group

Sint-Pietersnieuwstraat 41, 9000 Gent, Belgium

Label-free biosensors attempt to overcome the stability and reliability problems of biosensors relying on the detection of labeled molecules. We propose a label-free biosensor based on microring cavities in Silicon-on-Insulator (SOI) that fits in an area below $10x10\mu m^2$. *The resonance wavelength shift that occurs when the surroundings of a cavity is changed, is used for sensing. While theoretically the performance for bulk refractive index changes is moderate* (10^{-5}), *this device performs outstanding in terms of absolute molecular mass sensing (theoretical sensitivity of Ifg molecular mass) thanks to its extremely small dimensions. We use the avidin/biotin high affinity couple to demonstrate good repeatability and detection of protein concentrations down to 10ng/ml.*

Introduction

Optical label-free biosensors for protein detection attempt to overcome the drawbacks of commercialized microarrays, which rely on the detection of labeled molecules. This intermediate labeling step however complicates the detection process and decreases reliability. When biomolecular interaction takes place at the surface of an optical cavity, the resonance wavelength will shift. The semiconductor surface is chemically functionalized with receptor molecules that specifically interact with the target molecule. SOI offers a high refractive index contrast suitable for the fabrication of nanophotonic circuits including micron- and submicron sized optical cavities of very high quality. The enhanced light-matter interaction in a cavity increases the sensitivity while keeping the sensor's dimensions small [3]. Integrated in a microfluidic setup thousands of cavities can be lined up in arrays for multiparameter sensing within a few square millimeters.

SOI microrings for biosensing

Light with a wavelength $\lambda = \frac{n_{eff}L}{m}$, $m = 1,2,...$ resonates in a microring resonator with circumference L. This results in a sharp dip in the transmission. A change in the refractive index of the ring's environment shifts the resonance spectrum, which can be monitored by scanning the wavelength and by measuring the intensity profile at one well chosen wavelength. The sensitivity increases with increasing quality factors Q of the resonator. The Q-factor expresses the peak's width: $Q = \frac{\delta\lambda_{3dB}}{\lambda_{resonance}}$. Q-factors over 20,000 are easily achievable with our fabrication process and optimized design, the 3dB peak width is 75pm. Deep ultraviolet (UV)lithography, the technology used for advanced complementary metal-oxide-semiconductor (CMOS) fabrication offers both the required resolution and the throughput needed for commercial applications [1].

Measurements

Water with different sodium chloride concentrations is flown across the ring resonator in order to characterize the sensor for bulk refractive index sensitivity. Fig. 1a shows a linear shift of the resonance wavelength with increasing salt concentration of 70nm/RIU. The

variations are very small, proving a very high refractive index sensor's stability. A shift of one fifteenth of the peak width is easily measurable, so a minimal detectable wavelength shift of $5pm$ corresponds with a minimal detectable refractive index shift of 10^{-5} RIU.
In the present work we used the avidin/biotin system which has a high affinity constant and therefore has a stable and specific interaction, as a model of biomolecular interaction. Biotin was immobilized on the aminofunctionalized silicon surface. We compare the resonance wavelength of the cavity immersed in PBS, before and after being in contact with avidin solution (avidin in PBS), no bulk refractive index changes are involved. The evolution of the wavelength shift for different avidin concentrations compared to the reference PBS resonance wavelength is shown in Fig. 1b. For avidin concentrations above $10\mu g/ml$ the surface is fully covered, the resonance wavelength shift saturates. The estimated lowest detectable concentration, for a minimal detectable wavelength shift of 5pm, is $10ng/ml$. This compares well with commercially available label-free protein detection methods [2].
Measuring the output intensity at one wavelength is used for real time interaction detection. Graph 1c shows real time measurements for 10ng/ml and 50ng/ml avidin concentrations. The rise time is due to both the protein interaction rate and the mixing in the flow cell.

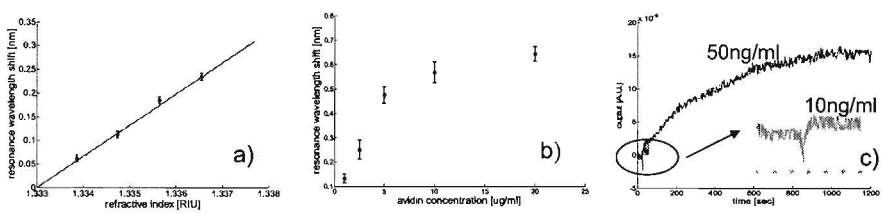

Figure 1: a) Resonance wavelength shift versus bulk refractive index change. b) Quantitative avidin/biotin detection with an SOI microring cavity. c)Real-time measurement of avidin/biotin interaction

Conclusions

We have demonstrated a highly miniaturized optical label-free biosensor based on a Silicon-on-Insulator microring cavity with Q factors over 20000. The refractive index sensitivity is 10^{-5} independent of the microring's radius. Measurements reveal proper operation of the device, being able to detect avidin concentrations down to 10ng/ml which compares favorably with commercial biosensing applications.

References

[1] W. Bogaerts et al., "Nanophotonic Waveguides in Silicon-on-Insulator Fabricated With CMOS Technology", *J. Lightwave Technology*, 2005, vol. 23, pp. 401.

[2] R. Ince, R. Narayanaswamy, "Analysis of the performance of interferometry, surface plasmon resonance and luminescence as biosensors and chemosensors," *Analytica Chimica Acta*,2006,vol. 569,p. 1-20.

[3] K. De Vos et al., "Optical Biosensor based on Silicon-on-Insulator Microring Cavities for Specific Protein Binding Detection," *Proceedings of SPIE Photonics West (Bios)*, 2007, p. 4667-19.

Design of a Spiral-Shaped Mach-Zehnder Interferometric Sensor for Refractive Index Sensing of Watery Solutions

M. Hoekman, M. Dijkstra, and H.J.W.M. Hoekstra

IOMS Group, MESA+ Research Institute, University of Twente,
P.O. Box 217, 7500 AE Enschede, The Netherlands.
e-mail: m.hoekman@ewi.utwente.nl, h.j.w.m.hoekstra@ewi.utwente.nl

The design of a spiral-shaped Mach-Zehnder Interferometric sensor (sMZI sensor) for refractive index sensing of watery solutions is presented. The goal of the running project is to realise a multi-sensing array by placing multiple sMZIs in series to form a sensing branch, and to place several sensing branches in parallel. In such an arrangment it is possible to use a single light source for several sensors. Each sensor will contain an electro-optical modulator, which makes it possible to separately interrogate and accurately read-out each sensor in the same sensing branch.

Introduction

The potential of the classical "straight" Mach-Zehnder Interferometric (MZI) sensor, as shown in Fig. 1, is large: the achieved resolution in refractive index changes obtained in the past at the IOMS group is in the order of $\delta N \sim 10^{-8}$ [1]. The two branches of the device are made as equal as possible to minimise the effect of fluctuations in temperature.

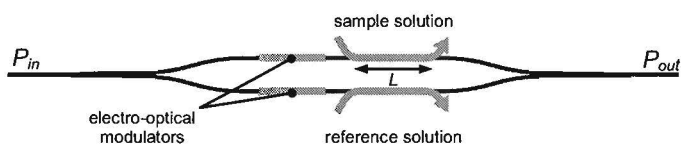

Figure 1. Top-view of a classical "straight" IO Mach-Zehnder Interferometer.

The straight MZI layout is not suitable for compact integration into multi-sensing arrays, mainly due to the device length (typically 4 cm). The large device length makes the sensor more vulnerable to process non-uniformities.

Spiral-shaped MZI layout

The goal of the running project [2] is to realise a multi-sensing array by placing multiple spiral-shaped MZIs in series to form a sensing branch, and to place several sensing branches in parallel, as is illustrated in Fig. 2. In such an arrangment it is possible to use a single light source for several sensors. Each sensor will contain an electro-optical modulator, which makes it possible to separately interrogate and accurately read-out each sensor in the same sensing branch.

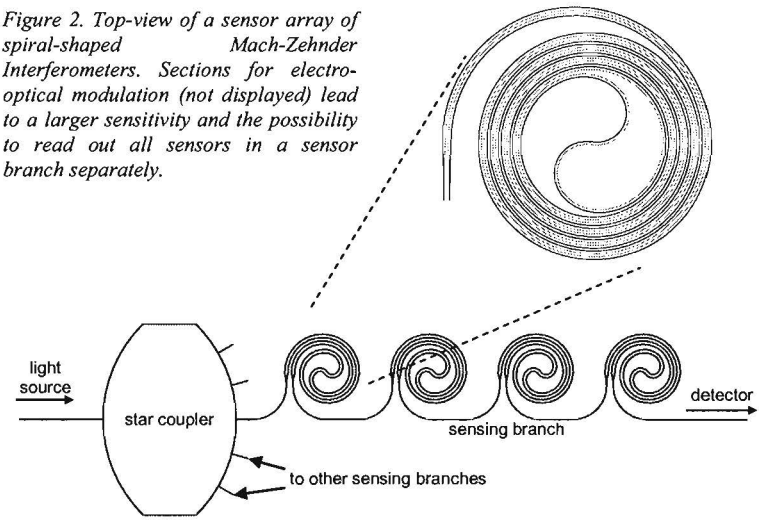

Figure 2. Top-view of a sensor array of spiral-shaped Mach-Zehnder Interferometers. Sections for electro-optical modulation (not displayed) lead to a larger sensitivity and the possibility to read out all sensors in a sensor branch separately.

The spiral-shaped layout of the MZI has several advantages: a long sensor window length can be placed in a compact sensor chip: within an area of 1 × 1 cm^2 lengths of several tens of centimeters are feasible. Moveover, the spiral shape has the advantage that if both MZI branches are identical (except for the sensor layer) the sensor should be very insensitive to temperature gradients across the chip. Another advantage is that the compactness owing to the spiral shape also allows cascading of several sensors.
A parametrised sMZI has been designed such that the position, slope, and curvature are continuous.

Photolithographically defined immunolayers

The sensors can each be coated with *e.g.* a specific immunolayer to be able to detect changes in concentration of viruses, bacteria or enzymes. In this project, technology is being developed for the immobilisation and photolithographical patterning of such immunolayers, which should result in a demonstrator to monitor the ripening process of cheese by measuring changes in the concentration of several different enzymes involved in this process.

Concluding remarks

A spiral-shaped MZI (sMZI) is being developed having the following features:

- Insensitivity for temperature gradients across the two branches
- Compact device layout
- Cascaded into multisensing arrays

References

[1] R.G. Heideman, P.V. Lambeck, "Remote Opto-Chemical Sensing with Extreme Sensitivity: Design, Fabrication and Performance of a Pigtailed Integrated Optical Phase-Modulated Mach-Zehnder Interferometer System", Sensors and Actuators B61, pp. 100 – 127, 1999.

[2] Acknowledgement: this research is being carried out within the framework of the STW project TOE.6596, "Multi-sensing arrays of separately accessible optics sensors".

POLIS-based fast All-Optical 2R Regenerator

C. Nambale, M.J.H. Marell, J.J.G.M. van der Tol

COBRA Research Institute, Eindhoven University of Technology,
Postbus 513, 5600 MB Eindhoven, The Netherlands

Introduction

Optical communication systems are an important part of today's communications networks which have to support bandwidth hungry applications like video, online games and peer-to-peer applications. Like in most communication channels, signal degradation occurs in fiber optic cables, the most common transmission channel for optical communication systems. Even with the latest fiber technology featuring transmission losses as low as 0.2-0.3 dB [1] per kilometer, repeaters are required every 50-100 km [2]. Repeated all-optical amplification of the signal leads to an accumulation of noise caused by amplified spontaneous emission (ASE). This means that at the very least 2R regeneration is required to reshape the signal thereby improving the optical signal to noise ratio (OSNR). Various methods and devices are currently used to regenerate the optical signal. Here we report a study on a 2R regenerator based on semiconductor optical amplifiers (SOA) that is realized using the POLarization based Integration Scheme (POLIS). POLIS combines active and passive components on the same material, using polarization properties of compressively strained InGaAs/InP quantum wells [3]. This study is carried out using numerical simulations with well known SOA rate equations [4] and those suggested by M. Marell [5] for the polarization converters (PC). Unlike the previous study [5] we are concentrating on the ultrafast effects in the SOA with a view to extending the applicability of the device to network speeds of up to 40 Gbps.

Preliminaries

2R regenerators based on SOAs have been extensively studied in many configurations involving Mach-Zehnder interferometers [6, 7, 8]. This study follows the same trend using a similar concept, however the interference in this regenerator is between two orthogonal polarizations induced by polarization converters in the POLIS structure. Figure 1 shows

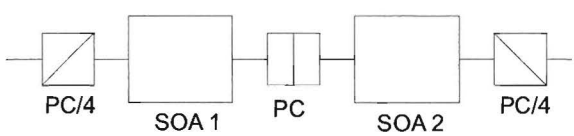

Figure 1: *2R regenerator*

a 2R regenerator with two partial polarization converters (PC/4) that split (on entry) or combine (on exit) the Transverse Electric (TE) and Transverse Magnetic (TM) polarizations. The full polarization converter (PC) switches the polarizations so that TE polarized light becomes TM polarized and vice-versa. The setup is such that, for signals that are not sufficiently strong (e.g. ASE noise contribution in a return-to-zero (RZ) digital system), the TE and TM polarizations will destructively interfere after traversing the regenerator

due to the $\pi/2$ phase shift introduced by (PC/4) and (PC) converter. Stronger signals (the logical 1's) will induce a phase change due to self-phase modulation in the two SOAs so that they are not 180° out of phase at the combining partial polarization converter.

Results

The transfer function of the setup mentioned above has been studied by M. Marell [5] and it agrees with the well known transfer function necessary for 2R regeneration.

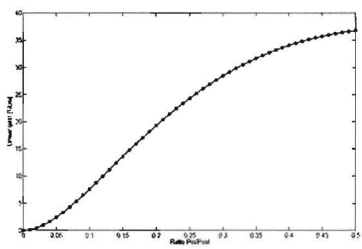

Figure 2: *2R regenerator transfer function*

Ultrafast nonlinear processes of the SOA have been studied using differential equations suggested by Mecozzi and Mørk [4]

$$\begin{aligned}
\frac{dh_N}{dt} &= -\frac{h_N}{\tau_s} - \frac{1}{S_s\tau_s}[G(t,z)-1]S(t,0) + \frac{g_0(z)}{\tau_s} \\
\frac{dh_{CH}}{dt} &= -\frac{h_{CH}}{\tau_{CH}} - \frac{\varepsilon_{CH}}{\tau_{CH}}[G(t,z)-1]S(t,0) \\
\frac{dh_{SHB}}{dt} &= -\frac{h_{SHB}}{\tau_{SHB}} - \frac{\varepsilon_{SHB}}{\tau_{SHB}}[G(t,z)-1]S(t,0) - \frac{dh_{CH}}{dt} - \frac{dh_N}{dt}
\end{aligned} \tag{1}$$

where ε_{SHB} and ε_{CH} are the nonlinear compression factors due to spectral hole burning (SHB) and carrier heating (CH) respectively. τ_s, τ_{CH} and $\tau_{SHB}$are the carrier lifetime, temperature relaxation time and carrier-carrier scattering times. h_N, h_{CH}, h_{SHB} are the modal gain contributions of carrier density, CH and SHB respectively.
The results show that there is sufficient phase change and recovery of the saturated gain to support speeds of up to 40 Gbps for miliwatt (mW) strength optical signals that are used in most optical communication systems.
The next step is to simulate the behavior of the optical pulses through the whole system and to calculate the improved OSNR and extinction ratio of a sequence of optical pulses.

Conclusion

The high speed operation of a 2R regenerator capable of operating in WDM systems at 40 Gbps is being studied. This regenerator occupies a smaller chip area than most 2R regenerators because of the use of a cascaded design as opposed to the Mach-Zehnder interferometer design which uses two arms.

Metal Grating Coupler for Silicon-on-Insulator

Stijn Scheerlinck, Jonathan Schrauwen, Frederik Van Laere, Dirk Taillaert, Dries Van Thourhout and Roel Baets

Photonics Research Group, IMEC-Ghent University,
Sint-Pietersnieuwstraat 41, 9000 Gent, Belgium
Stijn.scheerlinck@intec.ugent.be

Grating Couplers are a very elegant solution to the well-known coupling problem between single mode fibers and nanophotonic waveguides. In this paper, a novel type of grating coupler is introduced based on a metal grating. We discuss the design and, fabrication of metal grating couplers and present measurement results..

Introduction

Due to the large mismatch in mode size and shape between the fundamental mode of SOI waveguides and the mode of an optical fiber, coupling light efficiently from fiber to waveguide is rather challenging. Efficient and broadband grating couplers as compact as 10 μm x 10 μm have been proposed and demonstrated to solve this problem [1]. This device is based on etching a grating into the top silicon waveguide layer. In this paper, a different design is proposed and demonstrated. This novel type of grating coupler consists of a metal grating on top of the silicon waveguide layer.

Design

For the design of metal grating couplers and optimization, we use CAMFR, a two-dimensional fully vectorial simulation-tool based on eigenmode expansion and mode propagation with perfectly matched layer (PML) boundary conditions [2]. We consider 1-D gratings in 2-D simulations and concentrate on TE polarization (electric field parallel to the grating lines). With refractive index data for silver and gold taken from [3], the grating parameters (period, fill factor, height) were optimized to obtain high coupling efficiency. Another key parameter in the design of grating couplers is the buried oxide layer thickness. The result of this optimization is shown in Fig. 1, where the coupling efficiency is plotted as a function of buried oxide layer thickness for a silver grating with optimal grating parameters.

Fabrication and characterization

For the fabrication of prototype metal grating couplers, we had a few types of SOI wafers at our disposal. Based on the results of optimization discussed before, we choose to work with the SOI wafers with 2 micron buried oxide. Gold was chosen as the metal because of its inert chemical properties in contrast to silver which easily starts corroding after deposition. We studied two fabrication methods: (1) etching the grating in gold using a focused ion beam and (2) lift-off of gold after writing the grating in PMMA using e-beam lithography. Best results have been obtained using e-beam lithography. The main reason is that e-beam lithography does not require an intermediate protective layer as is the case for focused ion beam etching. As a proof-of-principle, a gold grating coupler was fabricated using e-beam lithography and lift-off on top of 10 μm wide SOI waveguides. They were characterized by fiber-to-fiber transmission measurements using the gold grating couplers to couple light in and out of the waveguide. A SEM-

image of the fabricated gold grating coupler on top of a waveguide is shown in the inset of Fig. 2, where the measurement data are plotted. For this prototype, a coupling efficiency of 20 % has been measured.

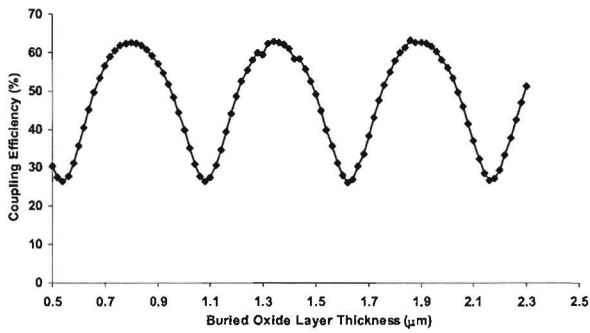

Fig. 1: Coupling efficiency of a silver grating coupler (period = 610 nm, fill factor = 30 %, height = 20 nm) as a function of buried oxide layer thickness.

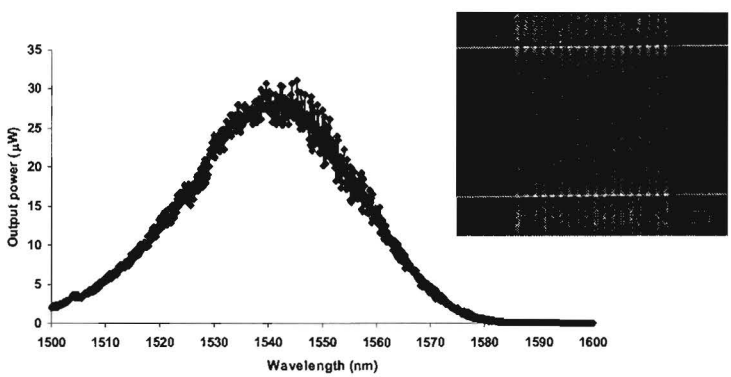

Fig. 2: Measurement data of fiber-to-fiber transmission via two gold grating couplers on top of a 10 μm wide SOI waveguide. Input power is set to 1 mW. Inset: SEM-picture of a gold grating coupler prototype. Bar length is 3 μm.

References

[1] D. Taillaert, F. Van Laere, M. Ayre, W. Bogaerts, D. Van Thourhout, P. Bienstman and R. Baets, "Grating couplers for coupling between optical fibers and nanophotonic waveguides," Jap. J. Appl. Phys. **45**, 6071-6077, 2006.

[2] P. Bienstman and R. Baets, "Optical modeling of photonic crystals and VCSEL's using eigenmode expansion and perfectly matched layers", Opt. Quantum Electron., **49**, 349-354, 2001.

[3] P.B. Johnson and R.W. Christy, "Optical Constants of the Noble Metals", Phys. Rev. B, **6 (12)**, 4370-4379, 1972

Polycrystalline silicon as waveguide material for advanced photonic applications

Shankar Kumar Selvaraja[1], Marc Schaekers[2], Wim Bogaerts[1], Dries Van Thourhout[1], Roel Baets[1]

[1] INTEC-IMEC, University of Gent, Gent, Belgium,
[2] IMEC, Leuven, Belgium

We report single mode polycrystalline silicon-on-insulator photonic wire fabricated in a CMOS fabrication facility. The optical quality and the material aspects of the polycrystalline-silicon for photonic application were studied. We report an optical propagation loss of 13.4dB/cm, which is the lowest loss reported for a 500nm wide photonic wire.

Introduction

With ever increasing complexity and density of photonic integrated circuits the need for multilayer functionality is arising for next generation photonic circuitry. Even though monocrystalline silicon-on-insulator exhibits superior optical quality it is difficult to realize multilayer circuitry based on this material, however, deposited Si is a very good candidate for such application. The deposited material can be amorphous or polycrystalline (poly) depending on the deposition technique and parameters. An optical loss of 9dB/cm has been demonstrated for broad (1-7μm) multimode photonic wires [1] fabricated in poly-silicon. In this work we have fabricated single mode photonic wires of 220nm thick and 500nm wide on poly-silicon deposited by a low pressure chemical vapor deposition (LPCVD) process. The effect of the material properties on the optical propagation loss was studied.

Design and Fabrication

Poly-silicon waveguides were fabricated on 200mm silicon handle wafers with 1μm of high density plasma (HDP) oxide as the bottom cladding/isolation followed by a chemical mechanical polish (CMP). Successively, a 220nm amorphous silicon layer was deposited by an LPCVD process at 560°C. Single mode photonic wires were then patterned by DUV lithography and etched using a $HBr/Cl_2/O_2$ gas chemistry. To reduce the rough sidewalls formed during the dry etch process, we grow a thin oxide layer. The oxide is grown at 900°C in an oxygen atmosphere. The photonic wires are then covered with HDP oxide as the top cladding followed by a CMP step. The oxide cladding serves as the isolation layer for any higher level circuitry. The oxide covered wafers are then annealed at 600°C for 30min to crystallize the amorphous silicon deposited by LPCVD. Unlike the work reported in [1] we use a short time and low thermal budget, which is important for fabrication in a production environment. The resulting poly-silicon is then hydrogenated in forming gas at 450°C to passivate the defects in the poly-silicon photonic wires.

Results and Discussion

Fig. 1 depicts the fabricated 500nm wide poly-silicon photonic wire. The photonic wires are fabricated with different length by spirals [2]. Light from a broad band source is

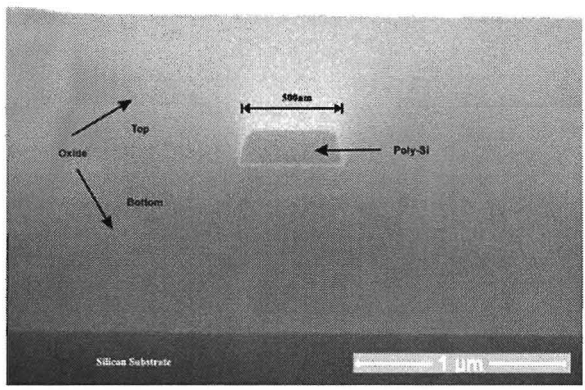

Figure 1Poly-silicon photonic wire with oxide as top and bottom clad

coupled into the photonic wire and the output at the other end is measured by a spectrum analyzer. Grating couplers were used at the input and output of the wires to couple light [2]. Samples were prepared with different process conditions to study the effect of the process on the optical loss. The effect of annealing, the oxide growth and hydrogenation were studied. The results show that high temperature annealing and hydrogenation are very important to make a photonic wire with decent propagation loss. The annealed and hydrogenated samples show a propagation loss of 13.4dB/cm. The losses for the samples without annealing or hydrogenation where too high to measure using our loss measurement technique. It was observed that growing a thin oxide of 2.5nm after etching decreases the loss by 3dB/cm; however, further oxidation increased the losses again. Various material analyses were done on the poly-silicon: atomic force microscopy, transmission electron microscopy and X-ray diffraction to study the roughness, grains and crystallinity respectively. The material analysis correlates with the optical loss mechanism.

Conclusion

Single mode poly-silicon photonic wires were fabricated. A propagation loss of 13.4dB/cm was measured, which is the lowest loss reported to our knowledge for a single mode poly-silicon photonic wire and which is acceptable for several photonic applications with micrometer scale footprint. The loss mechanism was analyzed through extensive material characterization. The results show the possibility for further reducing the loss below 13.4dB/cm.

Reference

[1] L. Liao, D. R. Lim, A. M. Agarwal, X. Duan, K. K. Lee and L. C.Kimerling, "Optical transmission losses in polycrystalline silicon strip waveguides: Effects of waveguide dimensions thermal treatment hydrogen passivation and wavelength", *J. Electron. Mater.* Vol. 29, no. 12, pp1380-1386, 2000.

[2] W. Bogaerts, P. Dumon, D. Van Thourhout, D. Taillaert, P. Jaenen, J. Wouters, S. Beckx, R. Baets, "Compact Wavelength-Selective Functions in Silicon-on-Insulator Photonic Wires", *IEEE J. Sel. Topics Quantum Electron.*, vol. 12, no. 6, pp. 1394-1401, 2006.

Cavity Solitons in Diffraction-Managed Optical Resonators

P. Tassin,[1] L. Gelens,[1] G. Van der Sande,[1] M. Tlidi,[2]
P. Kockaert,[3] J. Danckaert,[1] I. Veretennicoff[1]

[1]Department of Applied Physics and Photonics, Vrije Universiteit Brussel, Pleinlaan 2, B-1050 Brussel, Belgium

[2]Optique non linéaire théorique, Université Libre de Bruxelles, CP 231, Campus Plaine, B-1050 Bruxelles, Belgium

[3]Service d'optique et acoustique, Université Libre de Bruxelles, CP 194/5, 50 Av. F. D. Roosevelt, B-1050 Bruxelles, Belgium

We study optical resonators in which diffraction is controlled by use of a left-handed material. We show that it is possible to change the strength of diffraction due to the phase compensation between right-handed and left-handed materials in such systems. This control of diffraction allows decreasing the size of cavity solitons. However, when such cavity solitons become sub-diffraction-limited, other effects starts to dominate their spatial structure. We show that the inherent nonlocal interaction in left-handed materials imposes a new limit on the width of cavity solitons, which is nevertheless smaller than possible with a diffraction-limited system.

Introduction

Localised structures have been predicted and demonstrated in a variety of fields, such as chemistry, plant ecology, fluid dynamics, and optics [1]. These structures are formed due to the balance between nonlinearities (light-matter interaction), transport processes (diffraction, diffusion), and dissipation (absorption, cavity losses). Localised structures in optical systems – commonly referred to as cavity solitons – have been proposed as bright spots encoding information in all-optical data storage and processing.
However, the width of cavity solitons is a critical issue for such applications. In optical devices, their size is typically limited by diffraction. For example, in a microcavity semiconductor laser emitting light at $\lambda = 0.5$ μm, cavity solitons have been reported with a diameter of approximately 10 μm [2]. This corresponds to the calculated diffraction limit for this system. Note that the spot size is significantly larger than the wavelength due to the high photon lifetime in the resonant cavity.

Diffraction Management

Recently, we have devised a method to control the strength of the diffraction process by placing a left-handed material inside an optical resonator [3]. Such left-handed materials are artificially designed structures with negative effective permittivity and permeability.

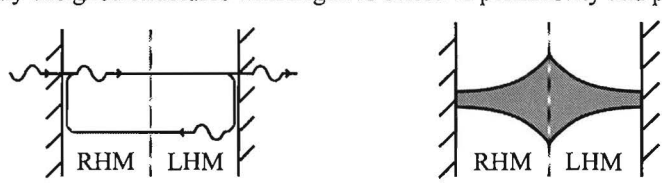

Figure 1: (left) An optical cavity with left-handed (LHM) and right-handed (RHM) material layers. (right) Phase compensation between both layers results in full or partial diffraction compensation.

Sub-Diffraction-Limited Cavity Solitons

In systems where diffraction is the dominating process governing the spatial dynamics, the width of cavity solitons typically scales as the square root of the overall diffraction strength. Therefore, the method of diffraction compensation described above, which allows making the diffraction strength as small as we want, would imply the generation of vanishingly small cavity solitons, beyond the limit imposed by natural diffraction.
Intuitively, however, it is clear that other spatially dependent processes will take over the role of diffraction. By careful analysis of the diffraction-compensated system, we have found that it is the nonlocal interaction in the left-handed material that will determine the spatial evolution of the field.

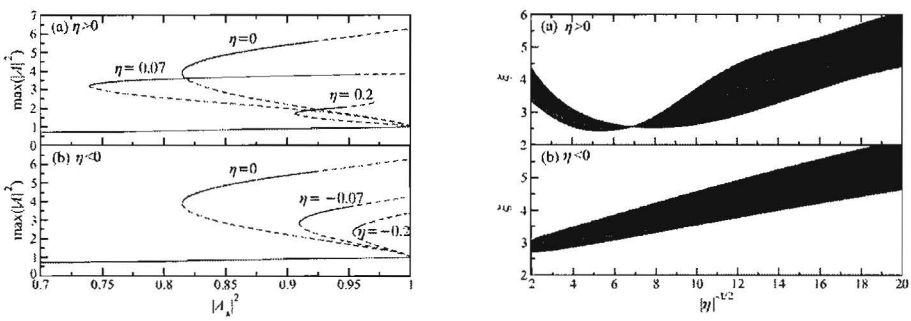

Figure 2: (left) Bifurcation diagrams for cavity solitons for several values of η, a parameter that measures the nonlocality strength relative to diffraction. (right) Diameter ξ of cavity solitons in function of η. Regions with stable (unstable) solitons are coloured blue (red).

Using a numerical analysis, we have investigated the influence of this nonlocal interaction on the existence and stability of cavity solitons. In Fig. 2 (left), we have plotted the bifurcation diagrams of the cavity solitons. We see that soliton branches emerge subcritically from the stable background. When diffraction is more and more compensated (higher η), the peak intensities are lowered, indicating a broadening of the cavity solitons. We also observe that for too high η (i.e., overcompensated), the stable part of the branches disappear.
In Fig. 2 (right), we have plotted the normalised width ξ of the cavity solitons. We see that the width decreases when diffraction is better compensated. However, when diffraction becomes too small, the cavity solitons width reaches a minimum for positive nonlocality ($\eta > 0$, upper part of the figure)), and saturates for negative nonlocality ($\eta < 0$, lower part of the figure). At the same time, the cavity solitons lose their stability when overcompensated. The nonlocal response of the left-handed material thus limits the size of cavity solitons. From a simple estimation, we find that the minimum width is about one wavelength.

References

[1] S. Trillo and W. Toruellas, Spatial Solitons, Berlin: Springer-Verlag, 2001.

[2] S. Barland, J. R. Tredicce, M. Brambilla, *et al.*, "Cavity solitons as pixels in semiconductor microcavities," Nature, vol. 419, pp. 699-702, 2002.

[3] P. Kockaert, P. Tassin, G. Van der Sande, I. Veretennicoff and M. Tlidi, "Negative diffraction pattern dynamics in nonlinear cavities with left-handed materials," Phys. Rev. A, vol. 74, 033822, 2006.

Optimization of a TM-mode Amplifying Waveguide Optical Isolator

W. Van Parys, D. Van Thourhout and R. Baets

Department of Information Technology, Ghent University (UGent),
Sint-Pietersnieuwstraat 41, 9000 Gent, Belgium. E-mail: wouter.vanparys@intec.UGent.be

An optical isolator that can easily be integrated with its source would significantly decrease the cost of a laser diode module. A promising scheme consists of an amplifying waveguide covered with a magnetized ferromagnetic metal. Earlier, we demonstrated this concept experimentally. Here we report on the optimization of the isolator. Magneto-optic waveguide calculations revealed a subtle interplay between the waveguide dimensions, the cladding material and the properties of the metal film. Our experimental result of 12.7dB optical isolation combined with full compensation of the internal loss is the best ever obtained. With this performance practical implementation is now within reach.

Introduction

An optical isolator is indispensable in a telecom link to protect laser sources against back-reflected light. A waveguide version of this component is highly desirable as it would decrease the packaging cost - hence the overall cost - of a laser diode module largely. An approach that is getting a lot of attention in recent years [1][2] involves the use of a ferromagnetic metal as the source of the non-reciprocal effect. In an optical waveguide covered with a transversely magnetized ferromagnetic metal film close to the guiding region, the magneto-optic (MO) Kerr effect induces a non-reciprocal shift of the complex effective index of the guided mode. Consequently, the modal loss is dependent on the propagation direction of the light. If the guiding core consists of amplifying layers, electrical biasing decreases the internal loss of the waveguide. The result is a device which, being transparent in the forward while providing loss in the opposite direction, is isolating. As the isolator basically has the same structure as the laser it is to be integrated with, monolithic integration is straightforward. This paper discusses the optimization of the TM-mode amplifying waveguide optical isolator.

Simulations

The performance of the amplifying waveguide optical isolator is obviously determined by the magneto-optic strength and the optical absorption of the ferromagnetic metal film and the amount of material gain that can be provided by the amplifying waveguide core. The optimization of both building blocks has been reported earlier [1]. The optimized heterostructure has a tensile strained AlGaInAs multi-quantum well core (9 wells with a thickness of 10nm) and is covered with a 50nm $Co_{50}Fe_{50}$ metal film.
Apart from these main building blocks the refractive index and the thickness of the cladding layers between the guided core and the metal film needs to be properly designed. A rough but very intuitive design rule can be stated like this: as the cladding thickness decreases, both the overall absorption in the metal and the non-reciprocal effect increase due to enhanced overlap of the light with the metal film. However, extensive study of the interaction of the waveguide mode with the metal revealed that the situation is much more complex. The actual non-reciprocal effect is determined by a subtle interplay between the

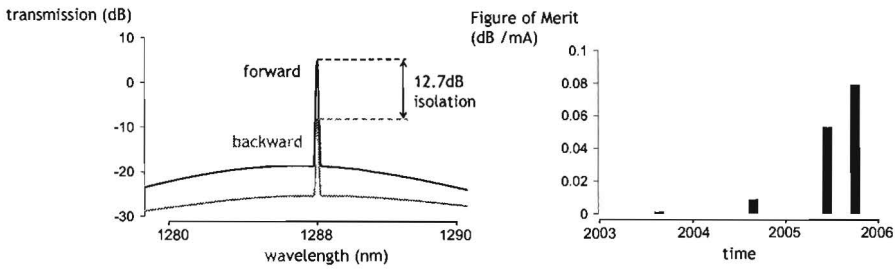

Figure 1: (left) Spectrum of the isolator transmission in both propagation directions, showing 12.7dB optical isolation - (right) Evolution of the demonstrated figure of merit with time.

phase of the (complex) electric field at the metal-semiconductor interface and the phase of the (complex) magneto-optic constants of the metal. It was only after taking this into account that the amplifying waveguide isolator layer structure could really be optimized.

Experimental Results

In figure 1 (left) a measurement example is shown. The transmission of a tunable laser signal through a 2mm long AR-coated isolator is plotted for both propagation directions. The device is electrically pumped with 160mA of current. The difference in transmission between the 'forward' signal and the 'backward' signal equals 12.7dB and the loss in the forward propagation direction is completely compensated (transmission $>$ 0dB). This result is the first demonstration of a transparent optical isolator that can straightforwardly be integrated with a semiconductor laser. In addition, the experimental isolation of 12.7dB is the highest value ever obtained on this kind of device.

Evolution Isolator Performance

Since the first experimental demonstration of the amplifying waveguide isolator mid 2003 [3], the device performance has continuously improved. This is illustrated in figure 1 (right). The suitable figure of merit (FoM) is the optical isolation (in dB) of a device requiring 1mA of current for forward transparency. In the three years that have passed since the first demonstration huge improvement of the FoM by a factor 80 has been achieved.

Conclusion

Improved understanding of the nature of the amplifying waveguide optical isolator resulted in a major advance of the state-of-the-art. We demonstrated the first transparent optical isolator, monolithically integratable with a laser source. The experimental isolation level of 12.7dB shows that practical implementation is now within reach.

References

[1] W. Van Parys et al., *Appl. Phys. Lett.*, 88, 071115 (2006).

[2] H. Shimizu et al., *J. Lightwave Technol.*, 24, pp.38-43 (2006).

[3] M. Vanwolleghem et. al, *Appl. Phys. Lett.*, 85(18), pp.3980-3982 (2004).

A Photonic Implementation of Reservoir Computing

K. Vandoorne, P. Bienstman

Photonics Research Group, Ghent University (UGent)

Sint-Pietersnieuwstraat 41, 9000 Gent, Belgium

Reservoir Computing[1] is a new approach to study and use Neural Networks, which try to mimic a brain-like intelligence. It uses memory and feedback in the reservoir to extract time correlated features and in this why it can solve complex classification and recognition tasks like speech processing[2]. This has already been realized using software but a hardware implementation needs yet to be realized. Photonics offers a good perspective to achieve this fast and economic.

Introduction

Neural Networks are networks that can be trained to solve complex classification and recognition problems. They mimic the nervous system in the brain, consisting of vertices which are interconnected end whereby every connection has a certain weight that can be adapted during the learning process. While feed forward neural networks (no feedback) are well studied and understood, they are unapt for solving problems with time dependence. Recurrent Neural Networks are better suited because they have memory due to the feedback loops, but they have been proven hard to train.

Recently a novel approach to these networks has been proposed: Reservoir Computing. The network is split up into two segments. The first one is the reservoir which is a RNN with random weights and which is further left untrained. The second one is the read-out function which will be trained to solve a specific problem. The idea is that by splitting up the functionality the read-out function can be kept simple and therefore easy to train, while the whole system keeps its interesting computational properties - like extracting time dependent features - thanks to the reservoir. This can be seen in figure 1.

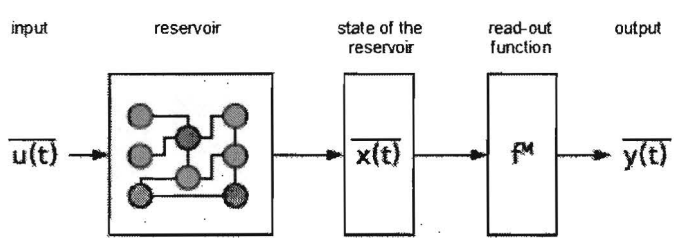

Figure 1: Reservoir computing

The implementation of Reservoirs has so far been restricted to software, so there is a need for a hardware implementation that performs in a power efficient way. Moreover the theory of Reservoir Computing doesn't limit the reservoirs to recurrent neural networks. Therefore a photonic implementation was proposed as a hardware implementation because it has properties which lead to a rich dynamical behaviour needed for reservoirs.

Photonics is the science which studies light and its interaction with materials. Nanophotonics tries to miniaturize the structures, needed to influence light, so that they would fit on a single chip. Given this it should be possible to develop a nanophotonic reservoir which is power efficient and very fast. It should be able to tacle all kinds of problems in an intelligent way, from the filtering of optical signals in telecom applications to speech recongition.

Implementation

The goal of this research is to develop a Reservoir based on nanophotonics. The reservoir will consist of different cavities which are interconnected. Inside the cavity non-linear effects will influence the properties of the resident light. These effects along with the degree of interconnection will determine the performance of the reservoir to solve complex problems. In a first stage the cavities will be studied until they are well understood. Different cavities will be evaluated like Photonic Crystal cavities (figure 2), Microdisklasers, SOA's,...
In the next stage they will be connected to form a reservoir. This reservoir will first be simulated and made into a hardware implemention to verify its computational potential.
The material system we are looking into is Silicon on Insulator (SOI) because it allows for compact designs and they can be made in collabaration with IMEC (Leuven). It will be necessary though to bond a layer of InP on the SOI[3] to enhance the non-linear effects, needed for a rich dynamic behaviour.

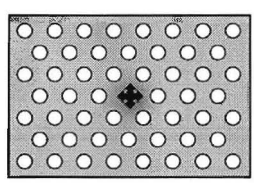

Figure 2: Photonic Crystal Cavity

Future work

In the near future the first reservoirs will be simulated and build to test their potential.

References

[1] W. Maass and T. Natschlger and H. Markram, "Real-time computing without stable states; a new framework for neural computation based on perturbations," *Neural Computation*, vol. 14, pp. 2531-2560, 2002.

[2] D. Verstraeten and B. Schrauwen and M. DHaene and D. Stroobrandt, "Isolated word recognition with the liquid state machine: a case study", in *Information Processing Letters*, 2005, pp. 521-528.

[3] G. Roelkens and D. Van Thourhout and R. Baets, "Ultra-thin benzocyclobutene bonding of III-V dies onto SOI substrates",Electronics Letters, 2005. pp. 561-562.

Author Index